Zn MOF 74 as pH responsive drug delivery system of arsenic trioxide

Jennifer Schnabel, Romy Ettlinger, Hana Bunzen

Angaben zur Veröffentlichung / Publication details:

Schnabel, Jennifer, Romy Ettlinger, and Hana Bunzen. 2020. "Zn MOF 74 as pH responsive drug delivery system of arsenic trioxide." *ChemNanoMat: Chemistry of Nanomaterials for Energy, Biology and More* 6 (8): 1229–36. https://doi.org/10.1002/cnma.202000221.

ACES Asian Chemical Editorial Society

DOI: 10.1002/cnma.202000221

CHEMNANOMAT
Full Paper

Zn-MOF-74 as pH-Responsive Drug-Delivery System of Arsenic Trioxide

Jennifer Schnabel, Romy Ettlinger, and Hana Bunzen*[a]

Abstract: Although arsenic and its compounds are mainly known as a poison, they also found applications as drugs in medicine. However, their distribution in a therapeutic dose is often problematic due to their high toxicity. One possibility how to address this issue is utilizing drug-delivery systems. Herein, we report on a metal-organic framework (MOF) called Zn-MOF-74, which comprises Zn(II) ions and 2,5-dihydroxybenzene-1,4-dicarboxylate ligands, as a drug nanocarrier of arsenic trioxide. We synthetized the material in a nanoparticle formulation and showed that due to the open metal sites in Zn-MOF-74, it was possible to load the material with a high amount of the As(III)-drug (in a form of arsenous acid). Moreover, we also investigated the drug release at different pH values. Noticeably, we observed that the As(III)-release was pH-triggered and was faster at pH 6.0 than at pH 7.4. Therefore, we suggest Zn-MOF-74 as a model example of a MOF containing open metal sites for controlled drug loading and delivery.

Introduction

Even though arsenic compounds are well-known as a poison, they have found several beneficial applications in medicine including cancer therapy.[1–3] For instance, in 2000 arsenic trioxide (As_2O_3) was approved by the U.S. Food and Drug Administration (FDA) as a drug for treatment of acute promyelocytic leukemia (APL)[4] and since 2016 the drug has also been approved by the European Medicines Agency (EMA).[5] Inspired by these approvals and positive therapeutic results of the drug in the APL treatment, since then arsenic trioxide has been tested as a drug to treat many other types of solid tumour entities including brain tumours, breast cancer and cervical cancer.[6–8] However, the usage of arsenic drugs in treatment of solid tumours is very challenging. In the treatment of APL (a cancer of the white blood cells), As_2O_3 is dissolved in a saline solution and given into a vein by injection. Thus, the drug concentration in the blood can be regulated by the dosage. Unfortunately, when treating solid tumours, it is often difficult to distribute the drug in a concentration sufficiently high to achieve the desired therapeutic effect at the targeted site, since increasing the dose of arsenic drugs is often not possible due to its high drug toxicity. One possibility, how to overcome this issue, could be using drug delivery systems (DDSs) for arsenic drugs.[9,10] DDSs represent a strategy of utilizing nanotechnology in medicine and up to now, several different types of materials have been suggested as drug nanocarriers. These include, for instance, carbon nanotubes,[11] dendrimers,[12] iron oxide nanoparticles,[13] gold nanoparticles,[14] liposomes,[15] mesoporous silica nanoparticles,[16] micelles[17] or quantum dots.[10,18] Utilizing nanoparticles for drug delivery offers many advantages over the conventional drug distributions such as improving drug stability and solubility, reducing drug side effects and enhancing the drug therapeutic efficacy.[9,10] For delivery of arsenic drugs, so far only few materials have been examined. These included liposomes,[7] polylactic acid-magnetic hybrid nanoparticles,[19] polyacrylic acid capped mesoporous silica nanoparticles[20] and magnetite doped mesoporous silica nanoparticles.[21] Recently, we contributed to the field by reporting on DDSs of arsenic drugs based on metal-organic frameworks.[22,23]

Metal-organic frameworks (MOFs) are crystalline porous materials comprising metal ions or clusters and organic ligands.[24] They have been shown to be an attractive class of materials with promising applications in many different areas including gas storage and separation,[25,26] catalysis,[27,28] sensing[29,30] and recently also in medicine.[31–33] Due to their large surface area (which enables a huge drug loading capacity), possibilities to modify their surface and their inherently biodegradable nature, MOFs seem to be perfect candidates for delivering drugs. In the last few years, there has been a huge progress in the field and many new examples of applications of MOFs in medicine have been reported.[32,33] These included stimuli responsive systems,[34,35] MOFs for photodynamic therapy,[36,37] theranostic applications,[38] or diagnosis.[39,40] Herein, we report on using a metal-organic framework called Zn-MOF-74 as a nanocarrier of arsenic trioxide. Zn-MOF-74 belongs to the well-known MOF-74/CPO-27 series and consists of Zn(II) ions and 2,5-dihydroxybenzene-1,4-dicarboxylate ligands.[41] Besides Zn-MOF-74, structural analogues with many other divalent metal cations – including Mg(II),[42] Mn(II),[43] Fe(II),[44] Co(II),[45] Ni(II)[46] and Cu(II)[47] – have been reported and have become one of the most extensively studied MOF systems. They have been

[a] J. Schnabel, R. Ettlinger, Dr. H. Bunzen
Chair of Solid State and Materials Chemistry
Institute of Physics
University of Augsburg
Universitaetsstraße 1, D-86159 Augsburg (Germany)
E-mail: hana.bunzen@physik.uni-augsburg.de

Supporting information for this article is available on the WWW under https://doi.org/10.1002/cnma.202000221

shown to be very promising materials for binding small molecules such as H_2, CO_2, CO and NO,[48] or for selective separation of gases or hydrocarbons.[49,50] The as-synthetized material comprises $[Zn_2(C_8H_2O_6)(solvent)_2]$ moieties that form a 3D honeycomb structure containing 1D hexagonal pores (Scheme 1). Each Zn(II) ion participates in a formation of six coordinate bonds - three with carboxylate groups, two with phenolate oxygen atoms and the last one is occupied by a solvent molecule (usually either water or DMF – depending on the synthesis conditions) which points into the channels. In order to enable guest binding, these solvent molecules can be removed postsynthetically, for instance, by applying elevated temperature and/or high vacuum, without altering the framework structure. Consequently, the desolvated MOF has a high density of vacant metal sites that are readily accessible for guest binding. MOFs with open metal sites turned out to be very useful materials for many applications including catalysis,[51] but also drug delivery.[52]

In DDSs the open metal sites can be used to bind drug molecules via a coordinate bond, i.e. in a very precise and defined manner. This aspect is particularly important when a delivery of toxic drugs is intended, i.e. in a situation when having a control over the drug dosage is essential. We recently showed that MOFs could be used as DDSs of arsenic drugs.[22,23] In these cases, the drugs were introduced to the system via a postsynthetic ligand exchange, i.e. some of the framework ligands were replaced by arsenic-containing ligands. Here we examined Zn-MOF-74 as a model example of a MOF with accessible metal open sites as a carrier of As_2O_3. Our motivation was to find out if it was possible to use a MOF with open metal sites for binding As(III)-species, and thus to achieve high drug loading (due to the high density of the open metal sites in the framework) and to get a control over the drug loading and release process. Last but not least, when considering MOFs as nanocarriers for drug delivery, the material toxicity has to be considered. It has been reported that the MOF-74 series exhibits only a very low toxicity.[53,54] For instance, Fe-MOF-74 nanoparticles have been shown to be non-toxic in PC12 cells.[53] In this work, we used Zn-MOF-74 which is based on low toxic components. It comprises zinc – i.e. an essential element with a lethal dose LD_{50} (rat, oral) of zinc nitrate hexahydrate equal to 1.190 mg/kg,[55] and 2,5-dihydroxybenzene-1,4-dicarboxylic acid as a ligand. The ligand belongs to a group of low molecular weight polyphenolics containing polyhydroxylated benzyl moiety that are abundant in medicinal plants,[56,57] and was shown to be non-toxic in human HCT116 cells.[56]

Results and Discussion

To fulfil the requirement of a drug delivery system, the following aspects were investigated and addressed: material synthesis in a nanoparticular formulation, chemical stability as well as As(III)-drug loading and release characteristics.

Material synthesis

If Zn-MOF-74 is used as a carrier of As(III)-drugs in cancer therapy, then an intravenous applications is intended. Therefore, it is important to keep the particle size in a nano-regime, ideally below 200 nm, in order to enable an accumulation of the material in cancer tissues via the enhanced permeability and retention effect[58] (i.e. a process in which nanoparticles small enough can leak out of the blood stream to cancer tissues which were found to have poorly defective endothelial cells compared to the cells in healthy tissues). Moreover, nanoparticles show better pharmacokinetic properties and systemic

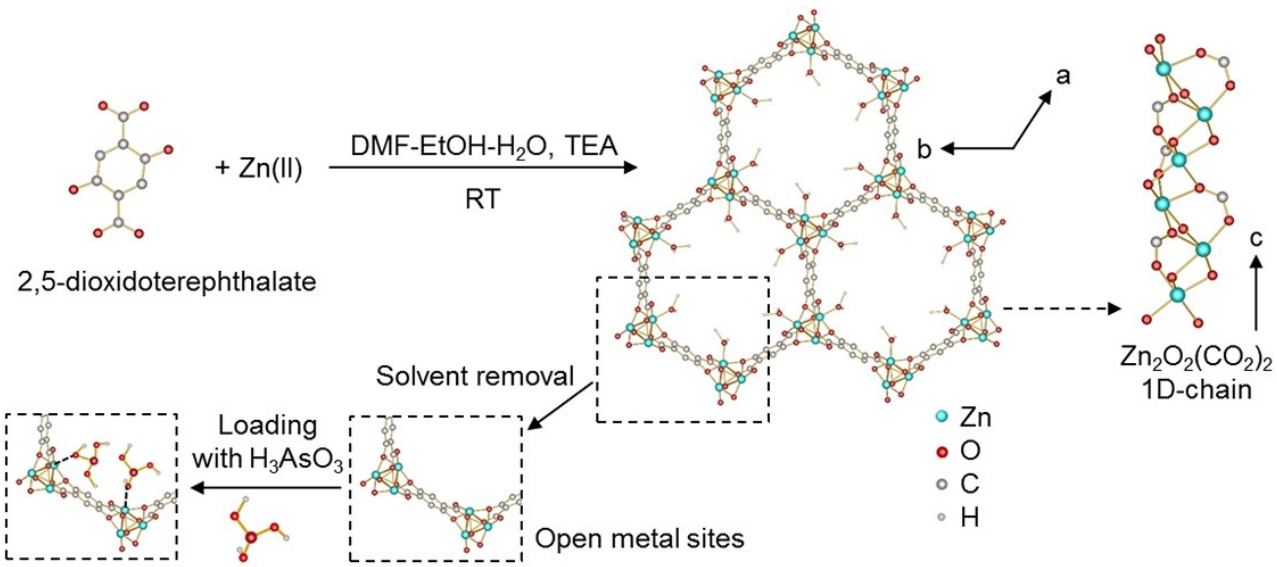

Scheme 1. Schematic representation of the synthesis and crystal structure of Zn-MOF-74 (CCDC: 265095) with a displayed honeycomb-like 1D pore channels and 1D-chains (along the *c*-direction), followed by the material activation and loading with H_3AsO_3. Based on experimental data, a binding mode for the drug loading was proposed and is schematically shown as a coordinate bond between the O-donor atom of $As(OH)_3$ and the Zn-cation.

circulation compared to bulk materials, and thus are advantageous as drug delivery systems.[9]

Nanoparticles of Zn-MOF-74 were synthetized according to the previously reported procedure.[59] Zinc nitrate hexahydrate was mixed with 2,5-dihydroxybenzene-1,4-dicarboxylic acid in a mixture of dimethylformamide, ethanol and water (25:3:3) and the mixture was stirred at room temperature until both solids dissolved (around 20 min). After that, trimethylamine (TEA) was added to the solution and the mixture was stirred for another 60 minutes. To remove any solvent molecules occluded inside the pores and those coordinated to the zinc ions, the sample was heated at 320 °C under vacuum (0.1 mbar) for 16 h. Both as-synthetized and activated materials were analysed by X-ray powder diffraction (XRPD) analysis, scanning transmission electron microscopy (STEM), Fourier-transform infrared (FTIR) spectroscopy and thermogravimetric analysis (TGA).

By comparing the XRPD patter of the synthetized sample to the calculated pattern obtained from single crystal XRPD analysis (CCDC: 265095),[41] it was confirmed that the synthetized material was a crystalline sample of Zn-MOF-74 (Figure 1). The diffraction peaks of the measured sample were broad which suggested a formation of nanosized crystals, which was further confirmed by STEM analysis (Figure 2). Additionally, we applied the Scherrer equation and calculated the crystallite size of the activated sample to be as small as 28.7 nm (for the calculation, three most intensive diffraction peaks in the region 5–20° were used).

To visualize the size and morphology of the Zn-MOF-74 particles, STEM micrographs were taken (Figure 2). These revealed globular around 100 nm large nanoparticles which was in agreement with the data reported in the literature for the same synthesis conditions.[59] To prove the successful solvent removal from the pores (both coordinated and non-coordinated molecules), TG curves (Figure 3) and FTIR spectra (Figure 4) of the material before and after the activation process were recorded. The TG analysis revealed that the mass loss below 200 °C corresponding to the solvent molecules disappeared after the sample activation (Figure 3) and in addition, the FTIR spectra showed that the characteristic ν(C=O) vibrational mode of DMF at 1654 cm^{-1} disappeared (Figure 4). Consequently, the data obtained by both analytical methods confirmed that the solvent molecules were successfully removed from the pores and thus, the coordination sites of the Zn(II) were made accessible for a guest binding.

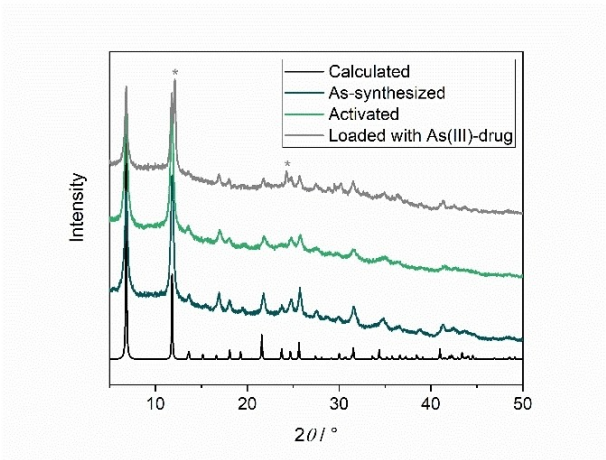

Figure 1. Measured and calculated XRPD-patterns of Zn-MOF-74 without and with the loaded As(III)-drug. Additional peaks found after the drug loading are marked with an asterisk *.

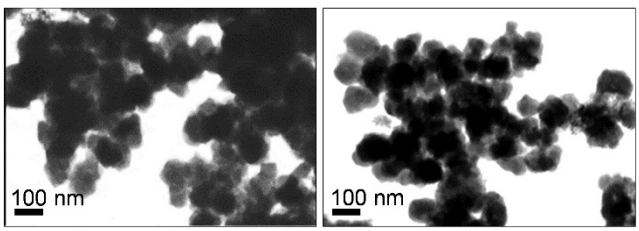

Figure 2. STEM micrographs of the Zn-MOF-74 nanoparticles before (left) and after the As(III)-drug loading (right).

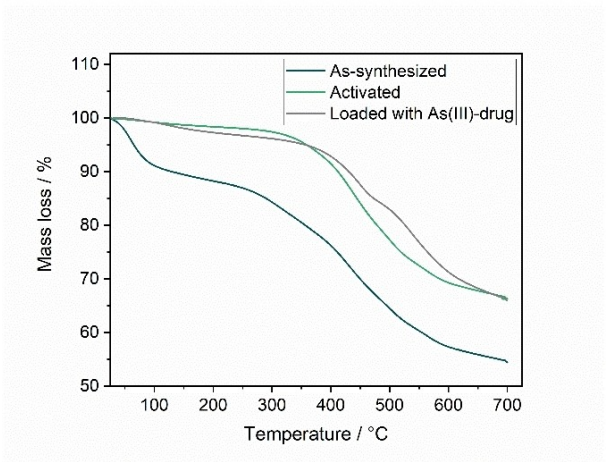

Figure 3. TG curves of Zn-MOF-74 before and after the As(III)-drug loading.

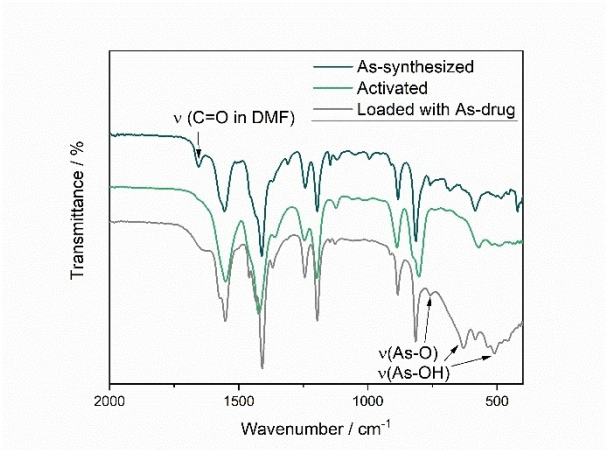

Figure 4. FTIR spectra of Zn-MOF-74 before and after the drug loading.

Drug loading

In order to load the As(III)-drug into the MOF nanocarrier, firstly sodium (meta)arsenite ($NaAsO_2$) – as a precursor of A_2O_3 with a high solubility in water - was dissolved in water. Depending on the pH-value, different anionic As(III) species can be obtained - $H_2AsO_3^-$ ($pK_{A1} = 9.22$), $HAsO_3^{2-}$ ($pK_{A2} = 12.10$) and AsO_3^{3-} ($pK_{A3} = 13.40$).[60] To optimize the loading conditions, we tested different pH-values (3, 6, 7.4 and 10) and times. We observed (by FTIR spectroscopy, Figure S1) that to achieve a successful loading, it was important to keep the pH value below 9.22 to make sure that the majority of the As(III)-drug is in a form of a neutral molecule (i.e. H_3AsO_3). However, if the pH was too low (here pH 3), the sample partly lost its crystallinity (Figure S2). Therefore, the highest drug loading, while preserving the sample crystallinity, was achieved at pH 6.0. This finding is in agreement with the recent work describing Zn-MOF-74 as an adsorbent for arsenic removal from water.[61] To increase the drug loading different times were tested (1.5, 4 and 24 h). However, prolonging the loading time from 1.5 h to 4 h did not result in an increased drug loading (determined by ICP-OES) and if the loading was carried out for 24 h, the sample crystallinity decreased (observed by XRPD, Figure S2). Therefore, to load the drug, we kept the activated nanoparticles in an aqueous solution of the drug at pH 6.0 for 1.5 h. The drug loaded MOF nanoparticles were analysed by XRPD, STEM, FTIR, TGA and elemental analysis (ICP-OES, inductively coupled plasma - optical emission spectrometry).

The XRPD analysis revealed two additional diffraction peaks at 12.07 and 24.20° (Figure 1) which suggested a successful coordination of the H_3AsO_3 drug to the accessible metal sites inside the pores. A similar observation was reported for Zn-MOF-74 with water molecules coordinated to the metal sites.[62] The presence of the As(III)-drug in the framework could be also detected by FTIR spectroscopy. According to literature,[63] adsorbed arsenous acid shows characteristic vibrational frequencies in the area between 800 and 500 cm^{-1}. And indeed, the FTIR-spectrum (Figure 4) of the As(III)-drug loaded Zn-MOF-74 revealed three additional bands at 759, 630 and 510 cm^{-1} in comparison to the original activated sample. These can be assigned to the vibration modes of (As–O) and (As–OH).[64] This also demonstrates that the As(III)-drug was in the pores in a form of H_3AsO_3 and not as As_2O_3 (shown in Figure S1). The existence of the hydrated form, which is usually stable only in a solution,[65] was possible due to the interaction with the framework. It was reported for the MOF MIL-100(Fe) that if $As(OH)_3$ was coordinated to the metal centre via the oxygen donor atom then a band around 800 cm^{-1} corresponding to the (As–O) vibration was detected.[66,67] If this band was missing, it was proposed that $As(OH)_3$ was bound to the framework via hydrogen bonding.[66] Another possibility could be that the $As(OH)_3$ drug is dissociated and protonates the phenolate oxygen atom of the ligand while being coordinated to the zinc centre as an arsenite anion ($H_2AsO_3^-$). However, this possibility was ruled out because we did not observe the vibration of the phenolic OH group of the ligand which was reported to be found in MOF-74 around 1333 cm^{-1}.[68] Based on these experimental data, we propose the binding mode showed in Scheme 1, where the As(III)-drug is bound to the MOF by a coordinate bond formed between the Zn(II)-centre and O-donor atom of $As(OH)_3$. Additionally, it is expected that the drug is further stabilized by hydrogen bonds formed between the drug and occluded water molecules.

To quantify the amount of the loaded As(III)-drug, elemental analysis was carried out. The As:Zn ratio was determined by ICP-OES as high as 0.29:1 (average value of three measurements). This corresponds to a loaded amount of 153 mg As_2O_3 in 1 g of the drug loaded MOF material (equivalent to 116 mg of elemental As in 1 g), which is significantly more than the As (III)-amount of the previously reported pH-responsive MOF nanocarrier called ZIF-8 (74 mg As per 1 g).[22] Nevertheless, with regard to the theoretical maximum loading capacity, which corresponds to a Zn:As ratio of 1:1, only 29% of the open metal sites in Zn-MOF-74 could be loaded with H_3AsO_3. This lower loading can be attributed to a completion in coordination by water ligands. This assumption was also confirmed by TG analysis (Figure 3) since a mass loss step (−3.3%) between 25 and 250 °C (attributed to the removal of water molecules) was detected. The drug binding was also reflected in the results of sorption analysis (Figure 5). The BET surface area of only 452 $m^2 g^{-1}$ was measured which was significantly lower than the reported value of 1187 $m^2 g^{-1}$ for an activated Zn-MOF-74.[69] Last but not least, the drug loaded material was investigated by STEM. STEM micrographs revealed that there were no changes to the particle size or morphology caused by the loading process (Figure 2).

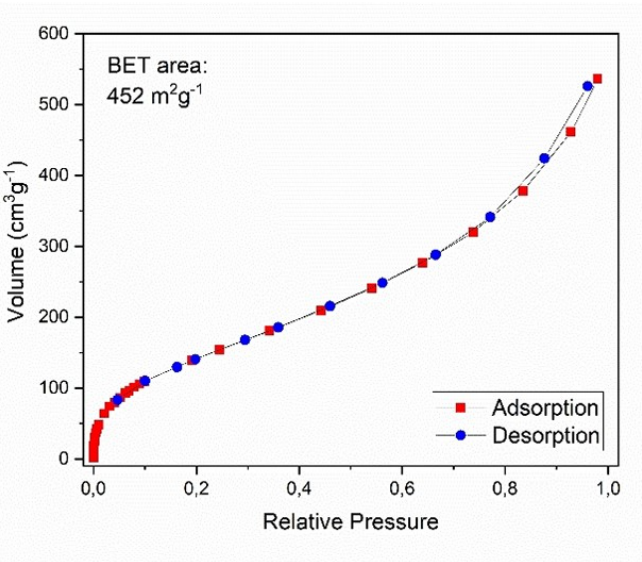

Figure 5. Argon adsorption isotherm of As(III)-drug loaded Zn-MOF-74 at 77 K.

Material stability and drug release

If a MOF is intended as a drug delivery system in cancer treatment, the material has not only to adsorb a high amount of a drug, but also to release it and the release should be preferably in a controlled manner. Optimally, the drug release should take place completely in an acidic pH often found in tumorous tissues (often around 6.0), while being as low as possible in the pH range of blood and healthy cells (around 7.4).[70] Therefore, both material stability and drug release were studied in these two pH values.

The material stability was studied by dispersing the As(III)-drug loaded material in a phosphate-buffered saline of two different pH-values – 6.0 and 7.4. The material was kept in the solution at 37 °C for 4, 24, 72 and 168 h. After the given period of time, the solid was isolated, washed well with water and investigated by XRPD analysis (Figure 6) and FTIR spectroscopy (Figure 7). The data from both analyses showed that Zn-MOF-74 was rather unstable at both tested pH values. At pH 7.4 the MOF was at least moderately stable for the first 4 hours, whereas at pH 6.0 the MOF decomposed quite rapidly, and we could not detect it after the first 4 hours by any of the two methods. The framework decomposition in both pH values resulted in a formation of zinc phosphate (formed by Zn ions released from the framework and phosphate ions from the buffer solution) as observed by both XRPD analysis and FTIR spectroscopy (Figure 6 and 7). At pH 7.4 in the FTIR-spectra vibration bands corresponding to the phosphate group $(PO_4)^{3-}$ were detected at 1026, 950 and 553 cm^{-1} and the XRPD analysis revealed the formation of $NaZn(PO_4 \cdot H_2O$. Noticeably, the crystalline phase of the phosphate salt was firstly detected after 3 days, suggesting that the material firstly transformed into an amorphous phase before the zinc ions were released. This was also confirmed by STEM images of the nanoparticles taken after 24 h of the drug release studies (Figure 9). At pH 6.0 a formation of a crystalline zinc phosphate was already detected after 4 h. In

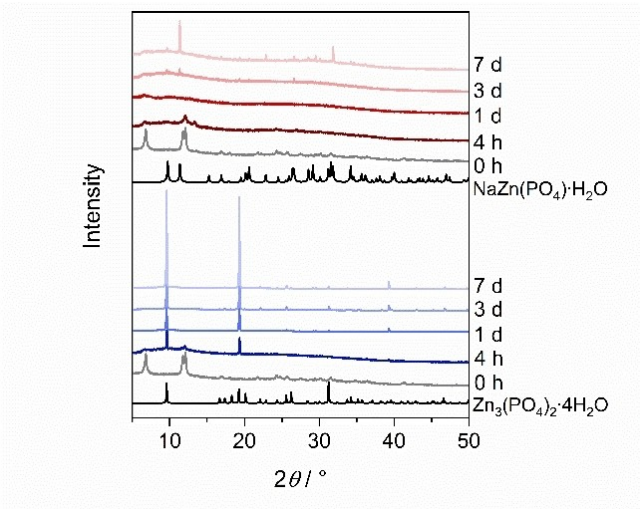

Figure 6. XRPD patterns of stability studies of Zn-MOF-74 loaded with H_3AsO_3, carried out in a phosphate buffered saline at pH 6.0 and pH 7.4, and their comparison to $Zn_3(PO_4)_2 \cdot 4H_2O$ (CSD: 18145) and $NaZn(PO_4) \cdot H_2O$ (CCDC: 81368).

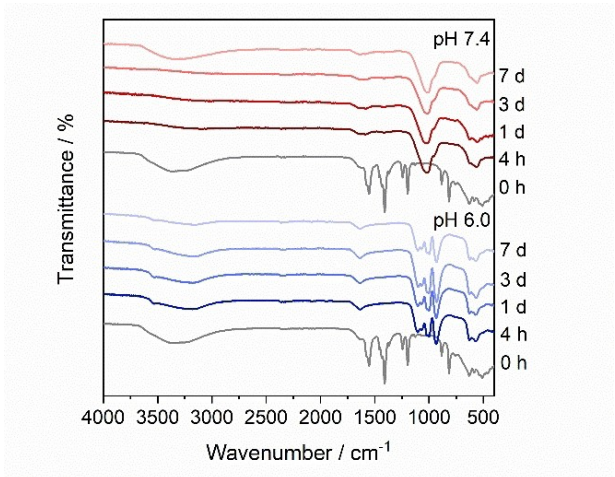

Figure 7. FTIR-spectra of stability studies of Zn-MOF-74 loaded with H_3AsO_3, carried out in a phosphate buffered saline at pH 6.0 and pH 7.4.

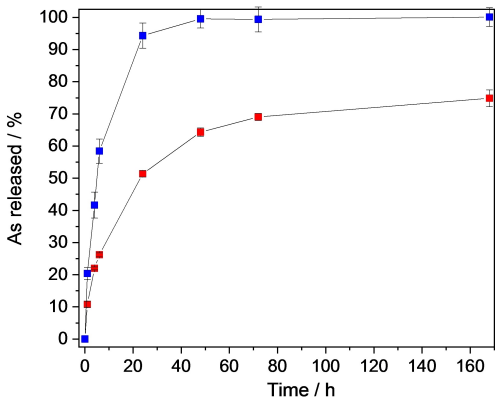

Figure 8. Arsenic release from the drug loaded Zn-MOF-74 at pH 6.0 (blue) and 7.4 (red) at 37 °C in phosphate-buffered saline, determined by ICP-OES.

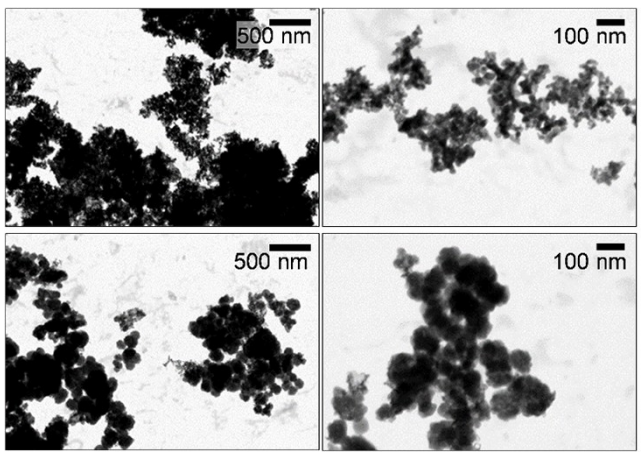

Figure 9. STEM micrographs of the drug loaded Zn-MOF-74 after 24 h at 37 °C at phosphate-buffered saline of pH 6.0 (top) and 7.4 (bottom).

the XRPD pattern the diffraction peaks of orthorhombic $Zn_3(PO_4)_2 \cdot 4H_2O$ (hopeite[71]) were detected. The phosphate formation was further confirmed by FTIR spectroscopy by detecting the vibration bands at 1102, 1071, 1003, 944 and 559 cm^{-1}.

To evaluate the drug release, the As(III)-drug loaded Zn-MOF-74 nanoparticles were dispersed in phosphate-buffered saline of two pH-values (6.0 and 7.4) and kept in the solution at 37 °C. The amount of arsenic and zinc ions released into the solution was determined after 1, 4, 6, 24, 48, 72 and 168 h by ICP-OES. In Figure 8 and Table 1 the arsenic release according to the time is shown. In the environment simulating a tumour tissue (i.e. at pH 6.0), the arsenic release was almost complete after 24 h with about 94.3 ± 3.9% of the originally loaded amount released. At pH 7.4, the arsenic release was significantly slower. After 24 h only about 51.4 ± 1.0% of arsenic was released and even after 7 days, the drug release was not complete. After 7 days, the remaining material still contained about 33.5 ± 0.1 mg of arsenic in 1 g, which corresponds to 28.93% of the originally loaded amount. On the other hand, at pH 6.0. the remaining amount of arsenic in the material after 7 days was only 1.1 ± 0.1 mg/g, which was less than 0.95% the original amount. Furthermore, not only the amount of arsenic but also the amount of zinc released to the solution was determined by ICP-OES. However, during the whole time period of the drug release tests, the detected amount of zinc in the solution was below 1% (Figure S3, Table S1) suggesting that the released zinc was fully consumed for the formation of phosphate salts. These results are in good agreement with the material stability studies, which showed that Zn-MOF-74 was more stable at pH 7.4 compared to pH 6.0 and that the material decomposition leads for both pH values to a release of zinc ions, which is followed by the formation of zinc phosphates (Figure 6 and 7). To visualize the material decomposition, STEM micrographs of the solid material after 24 h at pH 6.0 and 7.4 were recorded (Figure 9). The images revealed that indeed after 24 h at pH 6.0 the nanoparticles decomposed, whereas at pH 7.4 the nanoparticles were still detectable although not fully crystalline as shown by the XRPD analysis (Figure 7). The findings of the release studies are in agreement with the stability data reported for Zn-MOF-74.[68] In the study, the material stability was investigated as a function of vapour pressure and temperature. It was shown that the material decomposition was accelerated by a protonation of the phenolate oxygen atom of the ligand. Therefore, in a lower pH where the concentration of protons is higher, a faster material decomposition is expected. To further fine-tune the material stability and also biocompatibility, surface modification including polymer coating is possible.[72]

Table 1. Amount of arsenic (%) released from the As(III)-drug loaded Zn-MOF-74, determined by ICP-OES.

Time	pH 6	pH 7.4
1 h	20.4 ± 1.9	10.8 ± 1.0
4 h	41.6 ± 4.0	22.0 ± 0.5
6 h	58.4 ± 3.8	26.2 ± 0.6
24 h	94.3 ± 3.9	51.4 ± 1.0
48 h	99.5 ± 2.6	64.3 ± 1.3
72 h	99.4 ± 3.8	69.1 ± 1.1
168 h	100.0 ± 2.9	74.9 ± 2.6

The results of the arsenic release studies clearly showed that Zn-MOF-74 could be used as a drug carrier for pH-triggered drug delivery. Additionally, in comparison to the two previously reported MOFs for arsenic trioxide delivery: MFU-4 l (drug loading: 237 mg of As_2O_3/1 g; not pH-responsive)[23] and ZIF-8 (drug loading: 98 mg of As_2O_3/1 g; pH-responsive),[22] it combines the unique properties of both systems – it exhibits a high drug loading capacity (153 mg of As_2O_3/1 g) and features pH-triggered drug release.

Conclusion

In this work we showed that Zn-MOF-74 is a promising material for drug delivery of As(III) drugs. It fulfilled all the essential requirements for such a material – it could be synthesized in a nanoparticle formulation; it could be loaded with a high amount of arsenic (153 mg of As_2O_3 in 1 g of drug loaded material); and very importantly, it exhibited a pH-triggered release in a very favourable pH range for cancer therapy. The As(III)-drug was released faster at lower pH values, which is typical for the microenvironment of tumorous tissues, compared to pH 7.4, which is typical for healthy tissues. Our study also clearly showed that despite the MOF having large channel pores, it could be used for controlled drug loading and release due to the open metal sites. By this study we demonstrated that MOFs with open metal sites are highly promising materials for developing delivery systems of neutral drugs which, for instance due to their high toxicity, require a great control over the drug loading and release process. Inspired and encouraged by these positive results, we further plan to investigate porous materials with open metal sites and to carry out further tests with such materials including biological in vitro and in vivo tests.

Experimental Section

Materials and methods

All reagents were of analytical grade and used as received from commercial suppliers. The X-ray powder diffraction (XRPD) data were collected by using a Seifert XRPD 3003 TT- powder diffractometer with a Meteor 1D detector operating at room temperature using Copper K α_1Radiation ($\lambda = 1.54187$). The detected range of 2θ was from 4° to 50°. The Fourier-transform infrared (FTIR) spectra were recorded in the range of 400–4000 cm^{-1} with a measurement period of 32 scans on a Bruker Equinox 55 FT-IR spectrometer. The thermogravimetric analysis (TGA) was carry out with a Q500 analyser from TA Instruments in a temperature range from room temperature to 700 °C under nitrogen atmosphere at a heating grade of 10 K min^{-1}. The argon-gas sorption isotherm was measured with a Quantachrome Autosorb-I ASI-CP-8 instrument at 77.3 K in the range of $5.00 \times 10^{-5} \leq P/P_0 \leq 1.00$. The STEM micrographs were recorded on a ZEISS Crossbeam 550 operated at 30 kV. The samples were prepared by deposition a drop of the solid dispersed in ethanol onto carbon-coated copper

grids (200 mesh) and dried in air. The elemental composition of solid samples was determined by inductively coupled plasma optical emission spectrometry (ICP-OES) with a Vista MPX of VARIAN using arsenic and zinc standard solution of 10 ppm and 20 ppm.

Material synthesis

Zn-MOF-74: The MOF was prepared by following the procedure reported recently.[59] 0.950 g (3.19 mmol) of zinc nitrate hexahydrate and 0.405 g (2.04 mmol) of 2,5-dihydroxybenzene-1,4-dicarboxylic acid were mixed in a mixture of 25 mL of dimethylformamide (DMF), 3 mL of ethanol and 3 mL of water. The solution was stirred for 30 minutes in order to dissolve both solids. After that, 1.5 mL of trimethylamine (TEA) was added and the solution was stirred at room temperature for another 60 min. The formed solid was isolated with a centrifuge, washed twice with DMF and twice with dichloromethane, and dried on air overnight (0.750 g). To remove any solvent molecules occluded inside the pores and those coordinated to the metal ions, the sample was heated at 320 °C under vacuum (0.1 mbar) for 16 h. The product was analysed by XRPD, FTIR, STEM and TGA. FTIR (as-synthetized): $\nu = 1654$ (C=O, DMF), 1556, 1411, 1361, 1310, 1242, 1196, 1119, 883, 814, 584 cm^{-1}. FTIR (activated): $\nu = 1551$, 1422, 1360, 1245, 1198, 1113, 887, 801, 570 cm^{-1}.

Drug loading

An aqueous sodium (meta)arsenite solution (7.7 mM) was prepared by dissolving sodium (meta)arsenite $NaAsO_2$ (1 g, 7.7 mmol) in 1 L of distilled water and subsequent adjustment of the pH to 3, 6, 7.4 or 10 by either 1 M HCl or NaOH. The optimized drug loading conditions were as follows: the MOF material (200 mg) was dispersed in the As(III)-stock solution (200 mL) of pH 6 and kept in at room temperature without stirring for 90 min. After that, the solid material was isolated via centrifugation, washed well with water (three times) and dried at 65 °C overnight. The material was analysed by XRPD, FTIR, STEM, TGA and ICP-OES. FTIR: $\nu = 1552$, 1409, 1367, 1244, 1196, 1123, 883, 814, 795 (As–O), 630 (As-OH), 584, 510 (As-OH) cm^{-1}.

Material stability and drug release

To test the material stability and drug release, 0.01 M solutions of phosphate-buffered saline of pH 6.0 and 7.4 were prepared. In the material stability tests, 10 mg of the drug loaded material were dispersed in 10 mL of the phosphate-buffered saline (either of pH 6.0 or 7.4), and the suspension was kept at 37 °C without stirring for 4, 24, 72 or 168 h. After the given period of time the solid was isolated via centrifugation, washed well with water (3×5 mL) and analysed by FTIR and XRPD techniques.

In the drug release tests 10 mg of the drug loaded MOF were dispersed in 10 mL of the phosphate-buffered saline (either of pH 6.0 or 7.4). The suspension was kept at 37 °C without stirring. After a certain period of time (1, 4, 6, 24, 48, 72 or 168 h), 1 mL of the solution was carefully removed for analysis and replaced by 1 mL of fresh phosphate-buffered saline. The removed solution was filled up with 1 mL of concentrated nitric acid and 5 mL of distilled water and the amount of arsenic and zinc anions was determined by ICP-OES. Each release test was done in triplicates to prevent deviations.

Acknowledgements

The authors are grateful for financial support provided by the Else Kröner-Fresenius Foundation (project no. 2016_A181). Open access funding enabled and organized by Projekt DEAL.

Conflict of Interest

The authors declare no conflict of interest.

Keywords: metal-organic framework · arsenic trioxide · drug delivery · cancer therapy · nanoparticles

[1] A. Akhtar, S. Xiaoyan Wang, L. Ghali, C. Bell, X. Wen, *J. Biomed. Res.* **2017**, *31*, 177–188.
[2] D. Doyle, *Br. J. Haematol.* **2009**, *145*, 309–317.
[3] J. Hu, J. Fang, Y. Dong, S. Chen, Z. Chen, *Anti-Cancer Drugs* **2005**, *2*, 119–127.
[4] E. P. Swindell, P. L. Hankins, H. Chen, D. U. Miodragović, T. V. O'Halloran, *Inorg. Chem.* **2013**, *52*, 12292–12304.
[5] European Medical Agency (EMA), *Trisenox EMEA/H/C000388/II/0058 assessment report*, **2016**.
[6] K. Kerl, N. Moreno, T. Holsten, J. Ahlfeld, J. Mertins, M. Hotfilder, M. Kool, K. Bartelheim, S. Schleicher, R. Handgretinger, U. Schüller, M. Meister-ernst, M. C. Frühwald, *Int. J. Cancer* **2014**, *135*, 989–995.
[7] R. W. Ahn, F. Chen, H. Chen, S. T. Stern, J. D. Clogston, A. K. Patri, M. R. Raja, E. P. Swindell, V. Parimi, V. L. Cryns, T. V. O'Halloran, *Clin. Cancer Res.* **2010**, *16*, 3607–3617.
[8] Y. Du, D. Zhang, H. Liu, R. Lai, *BMC Biotechnol.* **2009**, *9*, 84.
[9] J. K. Patra, G. Das, L. F. Fraceto, E. V. R. Campos, M. D. P. Rodriguez-Torres, L. S. Acosta-Torres, L. A. Diaz-Torres, R. Grillo, M. K. Swamy, S. Sharma, S. Habtemariam, H.-S. Shin, *J. Nanobiotechnol.* **2018**, *16*, 71.
[10] S. Hossen, M. K. Hossain, M. K. Basher, M. N. H. Mia, M. T. Rahman, M. J. Uddin, *J. Adv. Res.* **2019**, *15*, 1–18.
[11] A. Bianco, K. Kostarelos, M. Prato, *Curr. Opin. Chem. Biol.* **2005**, *9*, 674–679.
[12] H. Wang, Q. Huang, H. Chang, J. Xiao, Y. Cheng, *Biomater. Sci.* **2016**, *4*, 375–390.
[13] H. Mok, M. Zhang, *Expert Opin. Drug Delivery* **2013**, *10*, 73–87.
[14] E. C. Dreaden, L. A. Austin, M. A. Mackey, M. A. El-Sayed, *Ther. Delivery* **2012**, *3*, 457–478.
[15] L. Sercombe, T. Veerati, F. Moheimani, S. Y. Wu, A. K. Sood, S. Hua, *Front Physiol.* **2015**, *6*, 286.
[16] A. Watermann, J. Brieger, *Nanomaterials* **2017**, *7*, 189.
[17] S. Cajot, D. Schol, F. Danhier, V. Préat, M.-C. Gillet De Pauw, C. Jérôme, *Macromol. Biosci.* **2013**, *13*, 1661–1670.
[18] R. Gui, A. Wan, Y. Zhang, H. Li, T. Zhao, *Anal. Chem.* **2014**, *86*, 5211–5214.
[19] X. Song, J. You, J. Wang, A. Zhu, L. Ji, R. Guo, *Chem. Res. Chin. Univ.* **2014**, *30*, 326–332.
[20] X. Xiao, Y. Liu, M. Guo, W. Fei, H. Zheng, R. Zhang, Y. Zhang, Y. Wei, G. Zheng, F. Li, *J. Biomater. Appl.* **2016**, *31*, 23–35.
[21] F. Muhammad, J. Zhao, N. Wang, M. Guo, A. Wang, L. Chen, Y. Guo, Q. Li, G. Zhu, *Colloids Surf. B* **2014**, *123*, 506–514.
[22] R. Ettlinger, N. Moreno, D. Volkmer, K. Kerl, H. Bunzen, *Chem. Eur. J.* **2019**, *25*, 13189–13196.
[23] R. Ettlinger, M. Sönksen, M. Graf, N. Moreno, D. Denysenko, D. Volkmer, K. Kerl, H. Bunzen, *J. Mater. Chem. B* **2018**, *6*, 6481–6489.
[24] O. M. Yaghi, M. O'Keeffe, N. W. Ockwig, H. K. Chae, M. Eddaoudi, J. Kim, *Nature* **2003**, *423*, 705–714.
[25] O. K. Farha, I. Eryazici, N. C. Jeong, B. G. Hauser, C. E. Wilmer, A. A. Sarjeant, R. Q. Snurr, S. T. Nguyen, A. Ö. Yazaydın, J. T. Hupp, *J. Am. Chem. Soc.* **2012**, *134*, 15016–15021.
[26] H. Li, K. Wang, Y. Sun, C. T. Lollar, J. Li, H.-C. Zhou, *Mater. Today* **2018**, *21*, 108–121.
[27] L. Zhu, X.-Q. Liu, H.-L. Jiang, L.-B. Sun, *Chem. Rev.* **2017**, *117*, 8129–8176.
[28] L. Jiao, Y. Wang, H.-L. Jiang, Q. Xu, *Adv. Mater.* **2018**, *30*, 1703663.
[29] L. Liu, Y. Zhou, S. Liu, M. Xu, *ChemElectroChem* **2018**, *5*, 6–19.

[30] L. E. Kreno, K. Leong, O. K. Farha, M. Allendorf, R. P. van Duyne, J. T. Hupp, *Chem. Rev.* **2012**, *112*, 1105–1125.
[31] G. Maurin, C. Serre, A. Cooper, G. Férey, *Chem. Soc. Rev.* **2017**, *46*, 3104–3107.
[32] C.-Y. Sun, C. Qin, X.-L. Wang, Z.-M. Su, *Expert Opin. Drug Delivery* **2013**, *10*, 89–101.
[33] M. Mozafari, *Metal-Organic Frameworks for Biomedical Applications;* Woodhead Publishing, **2020**.
[34] C.-Y. Sun, C. Qin, X.-L. Wang, G.-S. Yang, K.-Z. Shao, Y.-Q. Lan, Z.-M. Su, P. Huang, C.-G. Wang, E.-B. Wang, *Dalton Trans.* **2012**, *41*, 6906–6909.
[35] W. Cai, J. Wang, C. Chu, W. Chen, C. Wu, G. Liu, *Adv. Sci.* **2019**, *6*, 1801526.
[36] Q. Guan, Y.-A. Li, W.-Y. Li, Y.-B. Dong, *Chem. Asian J.* **2018**, *13*, 3122–3149.
[37] H. Zhang, Q. Li, R. Liu, X. Zhang, Z. Li, Y. Luan, *Adv. Funct. Mater.* **2018**, *28*, 1802830.
[38] H.-X. Zhao, Q. Zou, S.-K. Sun, C. Yu, X. Zhang, R.-J. Li, Y.-Y. Fu, *Chem. Sci.* **2016**, *7*, 5294–5301.
[39] P. Horcajada, T. Chalati, C. Serre, B. Gillet, C. Sebrie, T. Baati, J. F. Eubank, D. Heurtaux, P. Clayette, C. Kreuz, J.-S. Chang, Y. K. Hwang, V. Marsaud, P.-N. Bories, L. Cynober, S. Gil, G. Férey, P. Couvreur, R. Gref, *Nat. Mater.* **2010**, *9*, 172–178.
[40] X. Gao, Y. Wang, G. Ji, R. Cui, Z. Liu, *CrystEngComm* **2018**, *20*, 1087–1093.
[41] N. L. Rosi, J. Kim, M. Eddaoudi, B. Chen, M. O'Keeffe, O. M. Yaghi, *J. Am. Chem. Soc.* **2005**, *127*, 1504–1518.
[42] P. D. C. Dietzel, R. Blom, H. Fjellvåg, *Eur. J. Inorg. Chem.* **2008**, *2008*, 3624–3632.
[43] W. Zhou, H. Wu, T. Yildirim, *J. Am. Chem. Soc.* **2008**, *130*, 15268–15269.
[44] S. Bhattacharjee, J.-S. Choi, S.-T. Yang, S. B. Choi, J. Kim, W.-S. Ahn, *J. Nanosci. Nanotechnol.* **2010**, *10*, 135–141.
[45] P. D. C. Dietzel, Y. Morita, R. Blom, H. Fjellvåg, *Angew. Chem. Int. Ed.* **2005**, *44*, 6354–6358; *Angew. Chem.* **2005**, *117*, 6512–6516.
[46] P. D. C. Dietzel, B. Panella, M. Hirscher, R. Blom, H. Fjellvåg, *Chem. Commun.* **2006**, 959–961.
[47] R. Sanz, F. Martínez, G. Orcajo, L. Wojtas, D. Briones, *Dalton Trans.* **2013**, *42*, 2392–2398.
[48] K. Lee, J. D. Howe, L.-C. Lin, B. Smit, J. B. Neaton, *Chem. Mater.* **2015**, *27*, 668–678.
[49] Z. R. Herm, E. D. Bloch, J. R. Long, *Chem. Mater.* **2013**, *26*, 323–338.
[50] E. D. Bloch, L. J. Murray, W. L. Queen, S. Chavan, S. N. Maximoff, J. P. Bigi, R. Krishna, V. K. Peterson, F. Grandjean, G. J. Long, B. Smit, S. Bordiga, C. M. Brown, J. R. Long, *J. Am. Chem. Soc.* **2011**, *133*, 14814–14822.
[51] J. N. Hall, P. Bollini, *React. Chem. Eng.* **2019**, *4*, 207–222.
[52] L. Wang, M. Zheng, Z. Xie, *J. Mater. Chem. B* **2018**, *6*, 707–717.
[53] Q. Hu, J. Yu, M. Liu, A. Liu, Z. Dou, Y. Yang, *J. Med. Chem.* **2014**, *57*, 13, 5679–5685.
[54] S. Peng, B. Bie, Y. Sun, M. Liu, H. Cong, W. Zhou, Y. Xia, H. Tang, H. Deng, X. Zhou, *Nat. Commun.* **2018**, *9*, 1293.
[55] Sigma-Aldrich: http://www.sigmaaldrich.com/ (accessed Apr 2020).
[56] I. Kuriyama, Y. Nakajima, H. Nishida, T. Konishi, T. Takeuchi, F. Sugawara, H. Yoshida, Y. Mizushina, *Mol. Med.* **2013**, *8*, 535–542.
[57] M. Hatjimanoli, J. Favre-Bonvin, M. Kaouadji, A.-M. Mariotte, *J. Nat. Prod.* **1988**, *51*, 977–980.
[58] J. Fang, H. Nakamura, H. Maeda, *Adv. Drug Delivery Rev.* **2011**, *63*, 136–151.
[59] B. J. Abu Tarboush, A. Chouman, A. Jonderian, M. Ahmad, M. Hmadeh, M. Al-Ghoul, *ACS Appl. Nano Mater.* **2018**, *1*, 3283–3292.
[60] D. Mohan, C. U. Pittman, *J. Hazard. Mater.* **2007**, 142, 1–53.
[61] W. Yu, M. Luo, Y. Yang, H. Wu, W. Huang, K. Zeng, F. Luo, *J. Solid State Chem.* **2019**, *269*, 264–270.
[62] M. Sanchez-Sanchez, N. Getachew, K. Diaz, M. Diaz-Garcia, Y. Chebude, I. Diaz, *Green Chem.* **2015**, 17, 1500–1509.
[63] N. Y. Dzade, A. Roldan, N. H. de Leeuw, *Environ. Sci. Technol.* **2017**, *51*, 3461–3470.
[64] H. A. Szymanski, L. Marabella, J. Hoke, J. Harter, *Appl. Spectrosc.* **1968**, *22*, 297–304.
[65] A. Ramírez-Solís, R. Mukopadhyay, B. P. Rosen, T. L. Stemmler, *Inorg. Chem.* **2004**, *43*, 2954–2959.
[66] D. Wang, S. E. Gilliland, III, X. Yi, K. Logan, D. R. Heitger, H. R. Lucas, W.-N. Wang, *Environ. Sci. Technol.* **2018**, *52*, 4275–4284.
[67] J.-C. Yang, X.-B. Yin, *Sci. Rep.* **2017**, 7, 40955.
[68] K. Tan, S. Zuluaga, Q. Gong, P. Canepa, H. Wang, J. Li, Y. J. Chabal, T. Thonhauser, *Chem. Mater.* **2014**, *26*, 6886–6895.
[69] D. J. Tranchemontagne, J. R. Hunt, O. M. Yaghi, *Tetrahedron* **2008**, *64*, 8553–8557.
[70] I. F. Tannock, D. Rotin, *Cancer Res.* **1989**, *49*, 4373–4384.
[71] A. Whitaker, *Acta Crystallogr.* **1975**, *B31*, 2026–2035.
[72] R. S. Forgan, *Dalton Trans.* **2019**, *48*, 9037–9042.

Manuscript received: March 30, 2020
Revised manuscript received: April 27, 2020
Accepted manuscript online: May 28, 2020
Version of record online: June 16, 2020